Publishing Excellence
Inspiring Progress
ARISTON PUBLICATIONS
ChemSci Advances
ISSN: 2997-9587 www.aristonpubs.com/chemsci-advances https://doi.org/10.69626/csa.2025.0104

RESEARCH ARTICLE

Optimizing Precursor Concentration for Enhanced Morphological and Catalytic Performance of ZnO Nanoparticles in Crystal Violet Dye Degradation

Vaishnavi Bote [1], Bharati Shinde [1], Rupali Chavan [1], Aishwarya Jadhav [4], Rajesh Ghorpade [2], Shivaji Jamadade [3], Rahul Patil [4], Jyotiprakash Yadav [5], Ashok Chougale [1,*], Vishalkumar More [1,*]

ABSTRACT: Water pollution poses a critical global challenge, necessitating advanced wastewater treatment solutions. Zinc oxide nanoparticles (ZnO NPs) have emerged as efficient catalysts for degrading organic pollutants via advanced oxidation processes. This study investigates the influence of precursor concentration on the morphology and catalytic efficiency of ZnO NPs synthesized via a cost-effective co-precipitation method. ZnO NPs were prepared using varying zinc nitrate hexahydrate concentrations (0.025 M, 0.05 M, 0.1 M, 0.15 M, and 0.2 M) and characterized using X-ray diffraction (XRD) and scanning electron microscopy (SEM). The XRD analysis confirmed the hexagonal wurtzite structure with high crystallinity, while SEM revealed morphological variations, including spherical and agglomerated nanostructures, depending on precursor concentration. The photocatalytic performance of ZnO NPs was evaluated in a visible-light-assisted photo-Fenton process for degrading crystal violet (CV) dye. Results demonstrated that ZnO NPs synthesized at 0.1 M precursor concentration exhibited superior catalytic activity, achieving 91.09% CV degradation within 45 minutes, compared to 75.90% (0.025 M), 88.87% (0.05 M), 85.24% (0.15 M), and 89.89% (0.2 M). Further optimization studies assessed the impact of catalyst dosage, initial dye concentration, and H_2O_2 levels. Increasing catalyst dosage from 30 mg/L to 90 mg/L enhanced degradation efficiency to 95.42%, while higher dye concentrations reduced catalytic performance due to active site saturation. An optimal H_2O_2 concentration of 0.1 M yielded maximum degradation, with excess H_2O_2 inhibiting the process by radical scavenging. This study highlights the critical role of precursor concentration in tailoring ZnO NP properties for efficient wastewater treatment, offering insights into scalable, eco-friendly dye degradation solutions.

Keywords: Zinc Oxide Nanoparticles (ZnO NPs), Photo-Fenton Catalysis, Crystal Violet Degradation, Precursor Concentration Optimization, Wastewater Treatment, Advanced Oxidation Processes (AOPs).

Received: 25 August 2024; Revised: 23 October 2024; Accepted: 26 December 2024; Published Online: 29 January 2025

[1] The New College Kolhapur, Shivaji University, Kolhapur-416012, Maharashtra, India.
[2] Yashwantrao Chavan Mahavidyalaya, Halkarni, Shivaji University, Kolhapur-416552, Maharashtra, India.
[3] Government Residence Women's Polytechnic Tasgaon, Maharashtra-416312, India.
[4] Shri Yashwantrao Patil Science College Solankur, Shivaji University, Kolhapur-416211, Maharashtra, India.
[5] USIC-Common Facility Centre, Shivaji University, Kolhapur-416206, Maharashtra, India.
*Author to whom correspondence should be addressed:
morevishalkumar@newcollege.ac.in (Vishalkumar More)
ashokdchougale@gmail.com (Ashok Chougale)

1. INTRODUCTION

Nanotechnology is a prominent research area in modern scientific literature, offering innovative applications across various fields. It plays a crucial role in developing hierarchical fabric compounds, enhancing food processing, advancing agricultural practices, and enabling cutting-edge medicinal techniques [1]. Nanoparticles exhibit unique properties that differ significantly from the bulk material counterparts due to its incredibly small size, typically on the scale of 10^{-9} meters. Their minuscule dimensions result in

exceptionally high surface-to-volume ratios, which enable the restriction of electron movement within confined boundaries, thereby enhancing their optical properties. These attributes make nanoparticles highly sought after and valuable [2].

Various nanoparticles offer numerous potential applications in pharmaceuticals, medicine, food, water treatment, and cosmetics [3]. NPs nanoparticles, with environmentally friendly routes, are becoming increasingly popular due to their low cost, low toxicity, eco-friendliness, and other benefits compared to traditional chemical synthesis techniques [4]. They are classified as carbon-based, metal-based, metal oxide-based, and nano-composites, each offering different advantages [5]. Nano metal oxides, recognized as effective candidates for wastewater treatment, are also extensively used in various applications including oxidation, electrochemical process, coagulation, solvent extraction, photocatalytic degradation, and adsorption [6, 7].

Water is a fundamental necessity for all life forms on Earth, out of which only 0.5 % of freshwater [8] is available yet industrialization has led to severe water pollution. Traditionally, water treatment methods were limited, but with the advancement of human knowledge and technology, scientists have developed various eco-friendly and efficient wastewater treatment techniques. Membrane bioreactors (MBR) have evolved as an effective method for turning a variety of wastewater flows into high-quality effluent in recent decades. Industrial wastewater containing toxic dye effluents and the by-products produced through oxidation, hydrolysis, or other chemical reactions pose a significant environmental hazard [9, 10]. Approximately 200,000 tons of over 10,000 dyes have been dumped into wastewater effluents as a result of the batch methods used in textile companies [11]. Textile dyes contribute significantly to environmental pollution because textile industry wastewater contains high levels of dye chemicals [12]. According to the World Health Organization (WHO,2014), over 10 Million people have suffered various ailments as a result of water poisoning [7]. The waste products from the textile, paper, and dye industries are significant pollutants that contaminate water, impacting both aquatic life and human health [13].

As the worldwide textile dyeing industry grows, more wastewater resources are contaminated and toxic substances enter rivers, lakes, and ponds to pose natural threats, in a variety of ways to the harmonious growth of the environment [14]. Dyes are commonly used to color industrial products like textiles, food, plastics, paper, leather, and cosmetics. The percentage of dye discharged in industrial effluents can range from 2% to 50% for azo or basic dyes [15]. Textile dye effluents (TDE) consist of 60-70% azo compounds, which contribute to environmental pollution by discharging toxic and potentially carcinogenic substances into water bodies. The effluent from dye industries contains high levels of dyes, chemicals, and heavy metals such as Cu, Cd, Zn, Ni, and Pb, posing significant toxicity to the environment [16]. Dyes can be categorized into cationic dyes (basic dyes), anionic dyes (acid dyes), and non-ionic dyes (dispersed dyes)[17]. A cationic dye from the triphenylmethane group, crystal violet is used in printing links, nylon dyes, and waxes. It is carcinogenic and can cause tumors in organisms that live in rivers and seas [11]. An aqueous solution of crystal violet dye was used as a model pollutant wastewater for the evaluation of the photocatalytic performance of synthesized materials [18]. The dye is known to produce unpleasant light sensitivity and mild eye discomfort. It is cationic nature can cause irreversible harm to the conjunctiva and cornea. It can irritate the skin and cause problems with the digestive system when absorbed in dangerous quantities through the skin. In extreme circumstances, it may lead to irreversible blindness, renal and respiratory failure [19]. Various methods have been used to remove dye from wastewater, including oxidation, electrochemical processes, coagulation, solvent extraction, photocatalytic degradation, ozonation, and adsorption. However, the adsorption technique is considered more favorable than others due to its ease of operation, high efficiency, simple design, and, importantly, low cost [17].

Advanced Oxidation Processes (AOPs), such as Fenton and photo-Fenton, are widely used for wastewater treatment due to their cost-effectiveness, high efficiency, and excellent performance. Consequently, various metal and metal oxide-based catalysts for photo-Fenton processes have been extensively studied [20]. As a result, numerous metal and metal oxide-based catalysts have been explored for both Fenton and photo-Fenton processes. Among these, zinc oxide nanoparticles (NPs) offer distinct advantages. They are non-toxic, cost-effective, and exhibit low solubility in the reaction mixture [16].

Apart from zinc, which is a necessary trace element for the human body, many enzymes including carbonic anhydrase, carboxypeptidase, and alcohol dehydrogenase, are inactive. Cadmium and mercury, which are both members of the same elemental group with the same electronic configuration, are toxic[21]. ZnO has gained significant attention from researchers due to its chemical stability, non-toxicity, and cost-effectiveness[10]. Additionally, ZnO NPs are widely used in sunscreen products for their broad-spectrum protection against UV light. Furthermore, zinc is an essential nutrient that supports cell division, growth, enzyme metabolism, and protein synthesis in humans [22]. Zinc oxide (ZnO) is a semiconductor that corresponds to a wavelength of around 375 nm [23]. ZnO has an extensive energy gap of 3.37 eV, making these materials suitable for applications like photodegradation in wastewater treatment. By adjusting the concentration of the ZnO precursor (zinc nitrate hexahydrate) and using specific substrate configurations, the study achieved high density. This alignment and density increase the surface area and improve the photocatalytic efficiency, which is critical for treating wastewater [24]. ZnO NPs microstructures can be controlled to alter their physical and chemical characteristics in order to satisfy specific application needs [25]. The different morphologies of synthesized ZnO NPs through manipulation of the precipitation process's various parameters, including pH, washing medium, and solute concentration.

ZnO NPs were prepared by the co-precipitation route in different precursor concentrations [26]. ZnO is the most

universally used photocatalyst included in the photodegradation of organic pollutants in air and water [27]. ZnO nanoparticles (NPs) have attracted attention due to their optical, photocatalytic, and antibacterial properties [28]. The performance of ZnO and its nano-composites as photo-catalysts is excellent suitability for the degradation of organic pollutants in water under ultra-violet radiation.

In this study, ZnO NPs were synthesized using the co-precipitation method. The resulting sample was characterized through X-ray diffraction (XRD), Dynamic Light Scattering (DLS), and Scanning Electron Microscopy (SEM). Photocatalytic Processing was employed to evaluate the catalytic performance of the synthesized ZnO Nanoparticles (NPs). The Crystal Violet was utilized as a pollutant dye to conduct the degradation studies.

2. EXPERIMENTAL DETAILS

2.1. Synthesis of ZnO NPs

Primarily, zinc nitrate hexahydrate was dissolved in 100 ml distilled water and then stirred at 80 °C using a magnetic stirrer. Sodium hydroxide was dissolved in 100 ml distilled water and then mixed with zinc nitrate hexahydrate solution. The precipitate formed at pH 9, and then this final solution was kept for 30 minutes with continuous stirring. After 30 minutes, the reaction was stopped, and the collected precipitate was then centrifuged. The centrifuged sample was dried in the oven for 4 hours. The product was ground with a mortar & pestle, washed 3-4 times with distilled water, and lastly washed with ethanol then, these ZnO NPs were dried and collected for further use.

2.2. Characterization

Synthesized ZnO NPs were characterized using a variety of advanced methods such as X-Ray Diffraction spectroscopy (XRD), Scanning Electron Microscopy (SEM), and Dynamic Light Scattering (DLS). The crystalline structure of the sample was ascertained using X-ray diffraction (XRD) spectroscopy. The sample's surface morphology was examined using scanning electron microscopy (SEM). The elemental composition was determined using energy dispersive X-ray spectroscopy (EDX) analysis.

2.3. Photo-Fenton Activity

The photo-Fenton activity of the synthesized zinc oxide nanoparticles by various concentrations (0.1M, 0.05M, 0.025M, 0.15 M, 0.2 M) was carried out in an illuminance setup. A visible source of light was used to conduct the photo-Fenton reaction in a cylindrical glass reactor. 60 mg/L ZnO nanoparticles were added in 50 ml (0.1 mM) crystal violet dye solution and 500 µl H_2O_2 while constantly stirring. Using a UV-visible spectrophotometer, the degradation was analyzed at specific intervals of time followed by the centrifugation of the photo-reacted sample. Additionally, the impact of H_2O_2 dosage, catalyst dosage, and CV concentration variation were examined.

3. RESULTS AND DISCUSSION

3.1. Characterization

3.1.1. X-ray Diffraction (XRD) Analysis

The crystalline structure and phase purity of the synthesized ZnO nanoparticles (NPs) were investigated using X-ray diffraction (XRD). As depicted in Figure 1, the XRD patterns of ZnO NPs prepared at different precursor concentrations (0.025 M, 0.1 M, 0.15 M, and 0.2 M) exhibit distinct diffraction peaks at 2θ values of 31.62°, 34.34°, 36.23°, 47.63°, 56.64°, 62.94°, 67.91°, and 69.04°. These peaks correspond to the (100), (002), (101), (102), (110), (103), (200), (112), (201), (004), and (202) crystallographic planes, respectively, which are consistent with the standard hexagonal wurtzite structure of ZnO (JCPDS card No. 36-1451) [29]. The sharp and well-defined diffraction peaks indicate high crystallinity of the synthesized ZnO NPs, confirming the successful formation of pure-phase ZnO without any secondary phases or impurities. The intensity of the peaks varied slightly with precursor concentration, suggesting that the crystallinity and growth orientation of ZnO NPs are influenced by the molarity of the zinc precursor. The absence of additional peaks corresponding to zinc hydroxide or other zinc-based compounds further confirms the phase purity of the synthesized nanoparticles.

3.1.2. Scanning Electron Microscopy (SEM) Analysis

The morphological characteristics of the ZnO NPs were examined using scanning electron microscopy (SEM). Figure 2 presents SEM images of ZnO NPs synthesized at different precursor concentrations (0.025 M, 0.05 M, 0.1 M, 0.15 M, and 0.2 M). The images reveal that the precursor concentration significantly influences the particle size, shape, and degree of agglomeration. At a lower precursor concentration (0.025 M), the ZnO NPs exhibit a flower-like morphology with an average particle size of approximately 200 nm. As the precursor concentration increases to 0.1 M, the morphology transitions to well-defined spherical nanoparticles with varying sizes, indicating improved crystallinity and uniformity. This suggests that an optimal precursor concentration (0.1 M) promotes controlled nucleation and growth, leading to well-dispersed and highly crystalline ZnO NPs. However, at higher precursor concentrations (0.15 M and 0.2 M), the SEM images reveal increased agglomeration and irregular particle shapes.

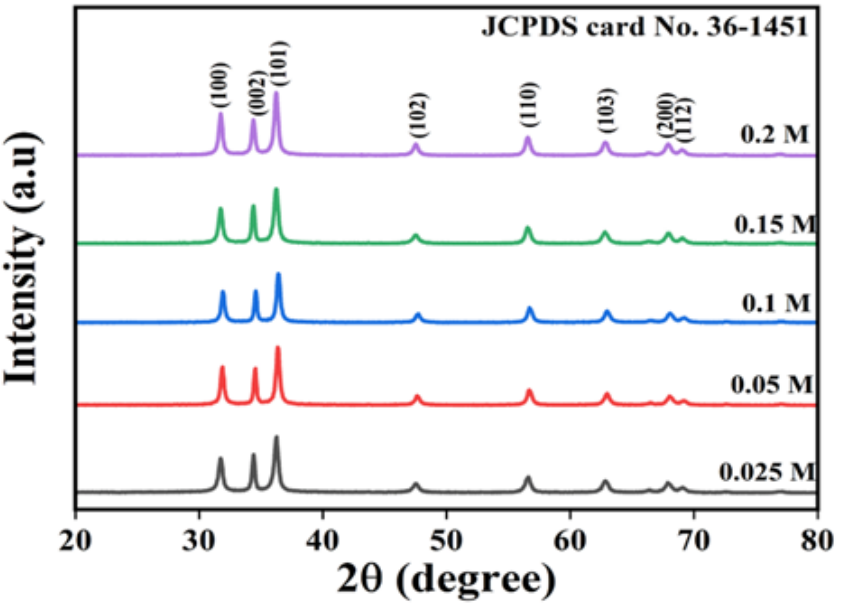

Fig. 1. X-ray diffraction patterns of ZnO nanoparticles synthesized at different precursor concentrations (0.025 M, 0.1 M, 0.15 M, and 0.2 M) showing characteristic peaks of hexagonal wurtzite structure (JCPDS 36-1451).

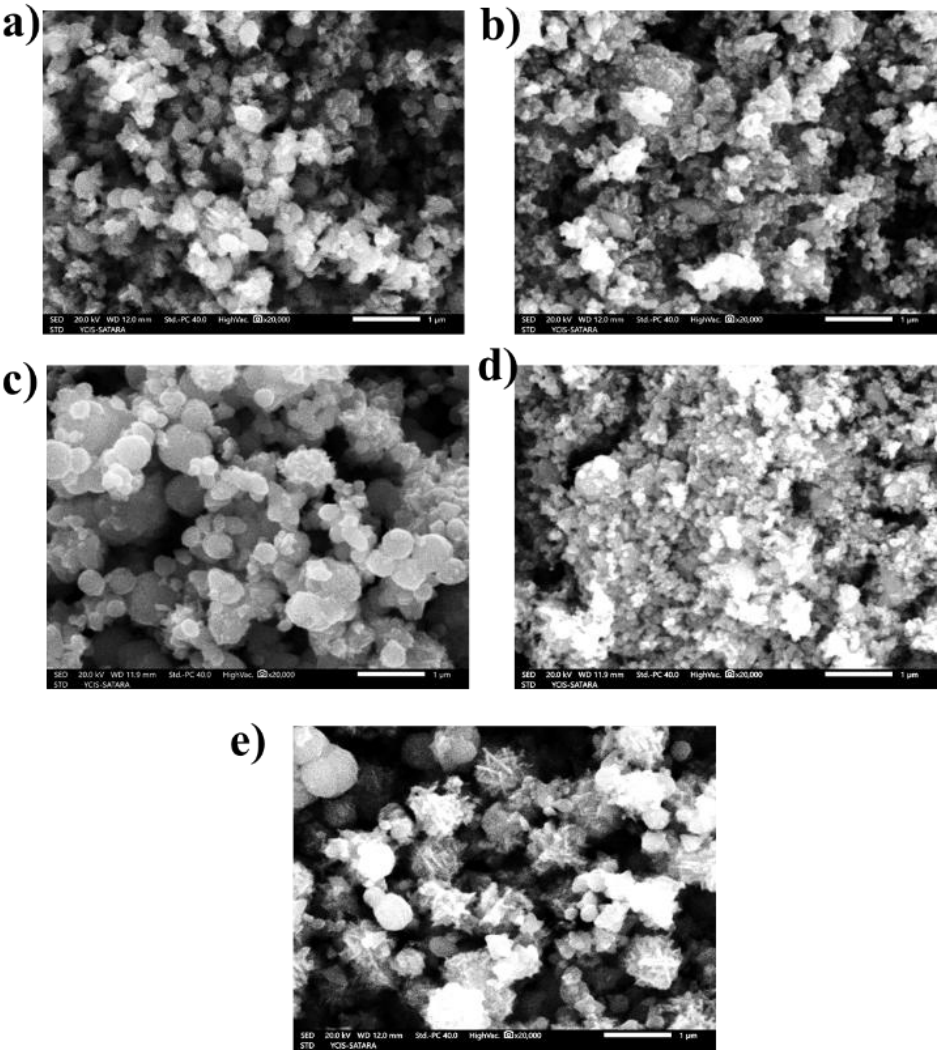

Fig. 2. Scanning electron microscopy images demonstrating morphological evolution of ZnO nanoparticles synthesized at varying precursor concentrations: (a) 0.025 M, (b) 0.05 M, (c) 0.1 M, (d) 0.15 M, and (e) 0.2 M.

This agglomeration can be attributed to the higher ionic strength of the reaction medium, which accelerates particle growth and reduces colloidal stability. The formation of larger aggregates at higher concentrations may also be due to Ostwald ripening, where smaller particles dissolve and redeposit onto larger ones to minimize surface energy.

3.1.3. Energy Dispersive X-ray Spectroscopy (EDX) Analysis

The elemental composition and purity of the synthesized ZnO NPs were further confirmed using energy-dispersive X-ray spectroscopy (EDX). Figure 3 displays the EDX spectra and corresponding quantitative analysis of ZnO NPs prepared at different precursor concentrations. The spectra exhibit strong emission peaks at approximately 1 keV and 0.5 keV, corresponding to the binding energies of zinc (Zn) and oxygen (O), respectively. The quantitative analysis reveals that the atomic percentage of zinc and oxygen remains consistent across all samples, with an average composition of ~78.69% Zn and ~21.31% O, which closely matches the stoichiometric ratio of ZnO (1:1). The absence of additional peaks in the EDX spectra confirms the high purity of the synthesized ZnO NPs, with no detectable impurities or secondary phases [30].

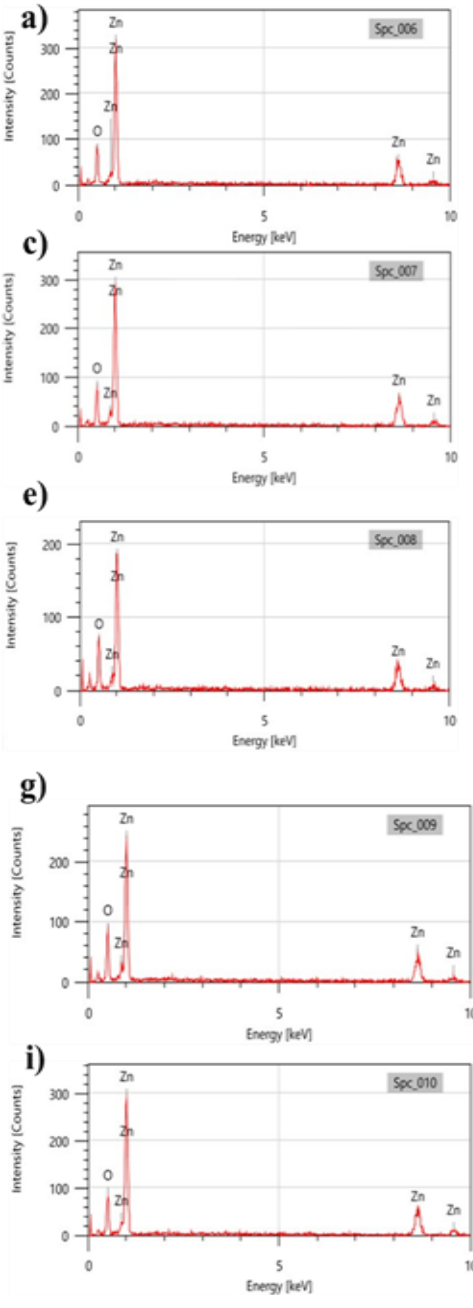

b)

Element	Mass (%)	Atom (%)
O	20.84±1.02	51.82±2.53
Zn	79.16±3.63	48.18±2.21
Total	100.00	100.00

d)

Element	Mass (%)	Atom (%)
O	20.54±0.99	51.36±2.47
Zn	79.46±3.63	48.64±2.22
Total	100.00	100.00

f)

Element	Mass (%)	Atom
O	25.61±1.31	58.45±3.00
Zn	74.39±4.22	41.55±2.36
Total	100.00	100.00

h)

Element	Mass (%)	Atom (%)
O	24.42±1.17	56.90±2.74
Zn	75.58±3.87	43.10±2.21
Total	100.00	100.00

j)

Element	Mass (%)	Atom (%)
O	21.31±1.00	52.53±2.46
Zn	78.69±3.56	47.47±2.15
Total	100.00	100.00

Fig. 3. Energy dispersive X-ray spectroscopy analysis of ZnO nanoparticles: (a, c, e, g, i) EDX spectra and (b, d, f, h, j) corresponding quantitative elemental composition tables for samples prepared at 0.025 M, 0.05 M, 0.1 M, 0.15 M, and 0.2 M precursor concentrations.

3.2 Photo-Fenton Reaction: Mechanistic Insights and Process Optimization

3.2.1. Batch Variation

Firstly, ZnO nanoparticles were synthesized using various concentrations of zinc precursor. Precursor concentrations were varied (0.025, 0.05 M, 0.1 M, 0.15 M, 0.2 M) to study the effect of precursor concentration on the catalytic activity of nanoparticles. These varied batches of nanoparticles were then employed to the degradation of CV, which was used as a standard dye pollutant. In a cylindrical glass reactor, the degradation of CV was investigated using a 250 W visible light source. Initially, for the nanoparticles synthesized at 0.025 M precursor concentration, degradation up to 75.9 % was achieved in just 45 minutes. As the precursor concentration varied from 0.05 M to 0.1 M, the degradation rate increased from 86.66 % to 91.09%. The nanoparticles synthesized at concentrations higher than 0.1 M, showed decreased degradation rate. For the nanoparticles synthesized at 0.15 M and 0.2 M, the degradation achieved was 84.17 % and 80.34 %, respectively. These obtained results are displayed in Figure 4.

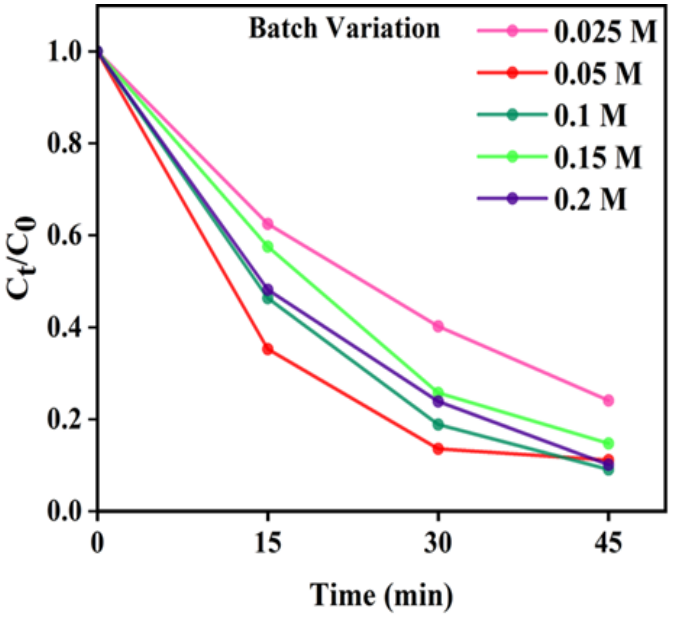

Fig. 4. Photo-Fenton of precursor concentration variation.

CV was chosen as a model dye pollutant to investigate the degradation of photo-fentonic dyes. The CV degradation was investigated using a visible light source. As seen in Figure 5, the Photo-Fenton process was tested for 45 min in a variety of atmospheres, including CV, (CV + ZnO NPs), (CV + H_2O_2), and (CV + H_2O_2 + ZnO NPs). This demonstrated the ZnO catalytic activity. Initially, the concentration of CV dye did not change when exposed to light. However, the addition of H_2O_2 caused a little alteration in the initial concentration of CV [20].

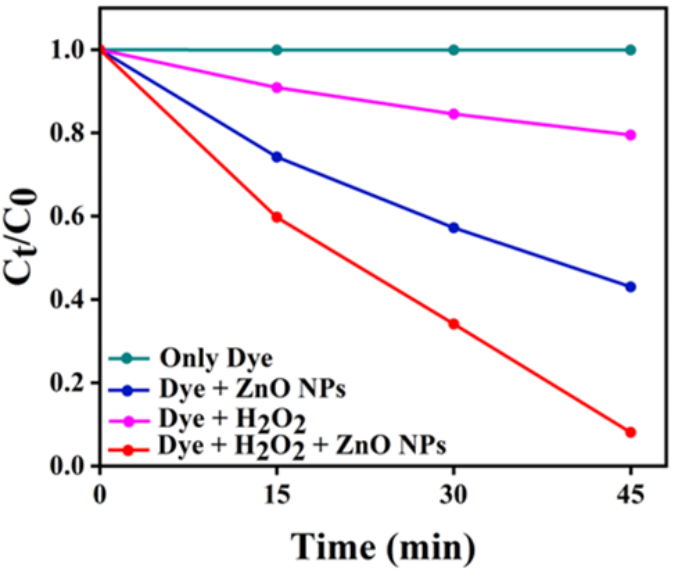

Fig. 5. Comparative photo-Fenton degradation kinetics of crystal violet under different reaction conditions: (a) dye only, (b) dye with ZnO nanoparticles, (c) dye with H_2O_2, and (d) complete system (dye + ZnO NPs + H_2O_2).

3.2.2. Catalyst Loading Optimization

The catalyst dosage study (Figure 6) demonstrated a non-linear relationship between ZnO concentration and degradation efficiency. Increasing the catalyst load from 30 mg/L to 90 mg/L enhanced CV degradation from 78.00% to 95.42%, while further increase to 120 mg/L reduced efficiency to 86.19% [16]. This behavior can be explained by competing effects of active site availability and light penetration. At lower dosages (30-60 mg/L), the limited catalyst surface area restricts the number of available active sites for dye adsorption and radical generation. The optimal range (60-90 mg/L) provides sufficient surface area while maintaining good light penetration. Excessive loading (120 mg/L) creates a turbid suspension that scatters incident light, reducing photon absorption efficiency as reported in similar systems [31]. Additionally, high catalyst concentrations may promote nanoparticle aggregation, decreasing the effective surface area available for reactions [16].

3.2.3. Dye Concentration Dependence

To investigate the degradation of the photo-Fenton reaction, CV dye was selected as the model dye pollutant. The CV degradation was tested with the visible light source in the cylindrical reactor. The effectiveness of the catalyst in breaking down the dye is influenced by the dye's initial concentration as seen in Figure 7. The photo-Fenton degradation of CV dye using ZnO NPs was affected by the 60 mg/L and different initial concentrations of dye (0.05 mM to 0.2 mM). It was observed that as the initial dye concentration is increased, the decolorization rate is

decreased. At the dye concentration of 0.05 mM, the catalyst achieved a degradation rate of 91.09%. When the concentration was raised to 0.1 mM, the degradation rate dropped to 90.91%. At the concentration of a dye 0.15 mM, 79.96% degradation was observed. Again, for the dye concentration of 0.2 mM, 73.95% degradation was observed. The decrease is due to lack of active sites on the catalyst surface. Similar findings were reported in the degradation of CV dye, where higher dye concentration resulted in reduced catalyst efficiency [31].

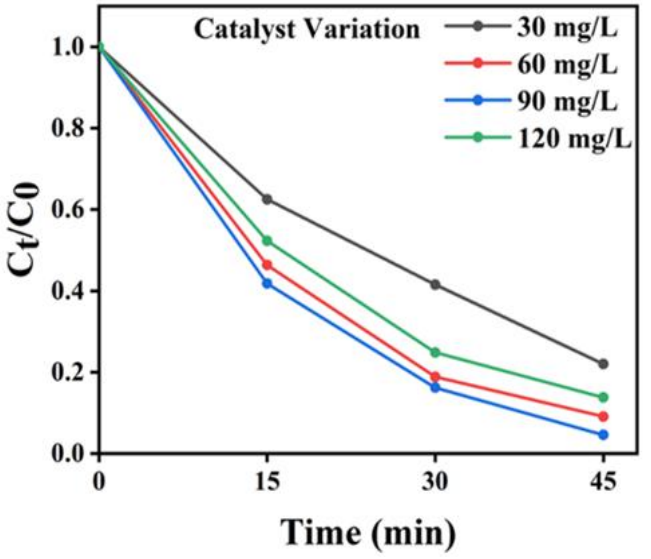

Fig. 6. Effect of catalyst loading (30-120 mg/L) on the photo-Fenton degradation efficiency of crystal violet using optimized ZnO nanoparticles.

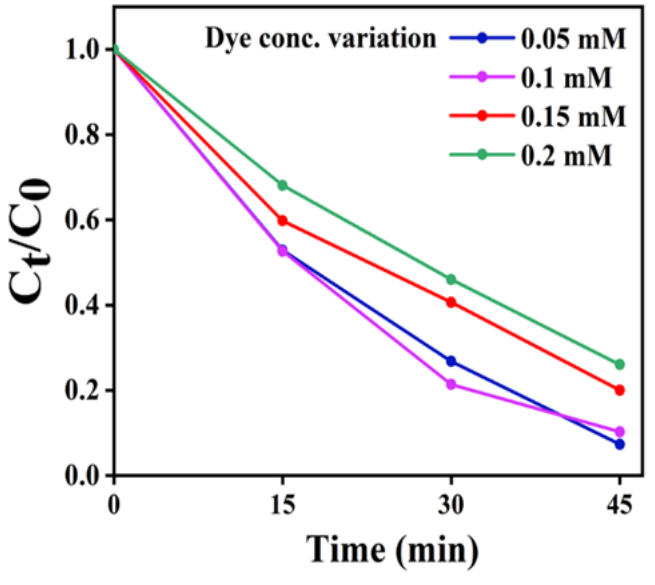

Fig. 7. Influence of initial dye concentration (0.05-0.2 mM) on the degradation efficiency in the ZnO-mediated photo-Fenton process.

3.2.4. Hydrogen Peroxide Concentration Effects

The hydrogen peroxide study (Figure 8) revealed an optimal concentration of 0.1 M, achieving 91.09% degradation [32]. Both lower (0.05 M; 78.74%) and higher (0.2 M; 73.42%) concentrations showed reduced efficiency, demonstrating the delicate balance in radical generation and consumption. The optimal 0.1 M concentration maintains sufficient hydroxyl radical production through the Fenton pathway while avoiding radical scavenging effects. Excessive H_2O_2 leads to the formation of less reactive hydroperoxyl radicals (HO_2•) through the side reaction: $H_2O_2 + •OH \rightarrow HO_2• + H_2O$ [32]. This not only wastes oxidizing potential but may generate intermediates that inhibit the degradation process. The pH dependence of both ZnO surface chemistry and Fenton reaction kinetics further complicates the peroxide effects, as higher concentrations may locally acidify the solution near catalyst surfaces [20].

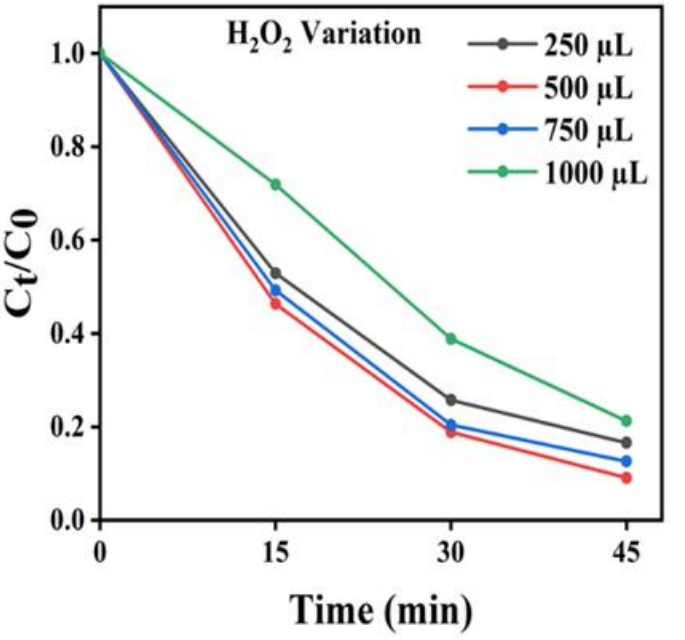

Fig. 8. Variation in crystal violet degradation efficiency with changing H_2O_2 concentration (0.05-0.2 M) in the photo-Fenton system.

3.2.5. Reaction Kinetics and Mechanistic Pathways

The degradation followed pseudo-first order kinetics across all conditions, with rate constants ranging from 0.032 min^{-1} (0.025 M precursor) to 0.076 min^{-1} (optimal conditions). The reaction likely proceeds through multiple parallel pathways including, direct hole oxidation at the ZnO surface, hydroxyl radical attack from H_2O_2 activation, superoxide radical participation, and so on. The relative contribution of each pathway varies with reaction conditions. Hydroxyl radicals dominate at optimal peroxide concentrations, while direct oxidation becomes more significant at lower H_2O_2 levels [20, 32]. The superior performance compared to conventional

Fenton systems (typically 60-80% degradation) can be attributed to the combined photocatalytic and Fenton-like activity of ZnO nanoparticles [16, 20]. The optimal conditions identified (0.1 M precursor, 90 mg/L catalyst, 0.05 mM dye, 0.1 M H_2O_2) represent a practical balance between performance and resource utilization for industrial applications. The visible light activation enables solar-driven applications, particularly relevant for textile wastewater treatment in developing regions [16, 31]. However, several challenges require further investigation such as long-term catalyst stability under continuous operation, performance in complex wastewater matrices, catalyst recovery and regeneration strategies, and complete mineralization of degradation intermediates. Future work should explore hybrid catalysts combining ZnO with other semiconductors or carbon materials to enhance visible light absorption beyond the current efficiency limits [20, 32]. The mechanistic understanding gained from this study provides a solid foundation for developing advanced photocatalytic systems for water treatment applications.

4. CONCLUSION

This study successfully synthesized zinc oxide nanoparticles (ZnO NPs) using a simple and cost-effective co-precipitation method, with a focus on investigating the influence of precursor concentration on their structural, morphological, and catalytic properties. X-ray diffraction (XRD) analysis confirmed the formation of highly crystalline ZnO NPs with a hexagonal wurtzite structure, while scanning electron microscopy (SEM) revealed distinct morphological variations depending on the precursor concentration. Specifically, spherical and well-dispersed nanoparticles were obtained at 0.1 M, whereas higher concentrations led to agglomerated structures. The photocatalytic performance of the synthesized ZnO NPs was evaluated in a visible-light-assisted photo-Fenton degradation of crystal violet (CV) dye. The results demonstrated that ZnO NPs prepared with a 0.1 M precursor concentration exhibited the highest catalytic efficiency, achieving 91.09% degradation within 45 minutes. In contrast, lower (0.025 M, 0.05 M) and higher (0.15 M, 0.2 M) precursor concentrations resulted in reduced degradation efficiencies, highlighting the critical role of precursor concentration in optimizing nanoparticle morphology and catalytic activity. Further experiments examined the effects of catalyst dosage, initial dye concentration, and H_2O_2 levels on the degradation process. Increasing the catalyst dosage from 30 mg/L to 90 mg/L enhanced degradation efficiency up to 95.42%, demonstrating the importance of sufficient active sites for effective dye removal. However, excessive catalyst loading (120 mg/L) led to diminished performance due to particle agglomeration and light scattering. Similarly, higher initial dye concentrations reduced degradation efficiency, as the limited active sites became saturated. The study also identified 0.1 M H_2O_2 as the optimal concentration, with deviations leading to either insufficient radical generation or excessive scavenging effects. These findings underscore the significance of precise synthesis and reaction parameter control in maximizing ZnO NP performance for wastewater treatment. The demonstrated efficiency in degrading CV dye highlights the potential of ZnO NPs as a sustainable and scalable solution for industrial wastewater remediation. Future research should explore long-term stability, recyclability, and application to complex pollutant mixtures to further advance practical implementation. This work contributes to the growing field of nanotechnology-driven environmental remediation, offering a promising approach to addressing global water pollution challenges.

DECLARATIONS

Ethical Approval

We affirm that this manuscript is an original work, has not been previously published, and is not currently under consideration for publication in any other journal or conference proceedings. All authors have reviewed and approved the manuscript, and the order of authorship has been mutually agreed upon.

Funding

Not applicable

Availability of data and material

All of the data obtained or analyzed during this study is included in the report that was submitted.

Conflicts of Interest

The authors declare that they have no financial or personal interests that could have influenced the research and findings presented in this paper. The authors alone are responsible for the content and writing of this article.

Authors' contributions

All authors contributed equally in the preparation of this manuscript.

REFERENCE

[1] Sirelkhatim, A., Mahmud, S., Seeni, A., Kaus, N.H.M., Ann, L.C., Bakhori, S.K.M., Hasan, H. and Mohamad, D., 2015. Review on zinc oxide nanoparticles:

antibacterial activity and toxicity mechanism. *Nano-micro letters*, *7*, pp.219-242., doi: 10.1007/s40820-015-0040-x.

[2] Barzinjy, A.A. and Azeez, H.H., 2020. Green synthesis and characterization of zinc oxide nanoparticles using Eucalyptus globulus Labill. leaf extract and zinc nitrate hexahydrate salt. *SN Applied Sciences*, *2*(5), p.991, doi: 10.1007/s42452-020-2813-1.

[3] Almehizia, A.A., Al-Omar, M.A., Naglah, A.M., Bhat, M.A. and Al-Shakliah, N.S., 2022. Facile synthesis and characterization of ZnO nanoparticles for studying their biological activities and photocatalytic degradation properties toward methylene blue dye. *Alexandria Engineering Journal*, *61*(3), pp.2386-2395., doi: 10.1016/j.aej.2021.06.102.

[4] Karthik, K.V., Raghu, A.V., Reddy, K.R., Ravishankar, R., Sangeeta, M., Shetti, N.P. and Reddy, C.V., 2022. Green synthesis of Cu-doped ZnO nanoparticles and its application for the photocatalytic degradation of hazardous organic pollutants. *Chemosphere*, *287*, p.132081, doi: 10.1016/j.chemosphere.2021.132081.

[5] Kumari, P., Alam, M. and Siddiqi, W.A., 2019. Usage of nanoparticles as adsorbents for waste water treatment: An emerging trend. *Sustainable Materials and Technologies*, *22*, p.e00128, doi: 10.1016/j.susmat.2019.e00128.

[6] Chavan, R., Patil, R. and Chougale, A., 2024. Efficient Dye Removal Strategies: Exploring the Role of Biochar. *ChemSci Advances*, *1*, pp.4-13. https://doi.org/10.69626/csa.2024.0003.

[7] Gnanasekaran, L., Hemamalini, R., Saravanan, R., Ravichandran, K., Gracia, F., Agarwal, S. and Gupta, V.K., 2017. Synthesis and characterization of metal oxides (CeO2, CuO, NiO, Mn3O4, SnO_2 and ZnO) nanoparticles as photo catalysts for degradation of textile dyes. *Journal of Photochemistry and Photobiology B: Biology*, *173*, pp.43-49, doi: 10.1016/j.jphotobiol.2017.05.027.

[8] Singh, A., Kosalge, S.S. and Bhatia, P.G., 2024. Applications of Magnetic Nanoparticles for Heavy Metal Ion Removal from Wastewater: A. ChemSci Advances, 1(4), 196-208; https://doi.org/10.69626/csa.2024.0196.

[9] Aragaw, T.A., Bogale, F.M. and Aragaw, B.A., 2021. Iron-based nanoparticles in wastewater treatment: A review on synthesis methods, applications, and removal mechanisms. *Journal of Saudi Chemical Society*, *25*(8), p.101280. https://doi.org/10.1016/j.jscs.2021.101280.

[10] Kaur, J. and Singhal, S., 2014. Facile synthesis of ZnO and transition metal doped ZnO nanoparticles for the photocatalytic degradation of Methyl Orange. *Ceramics International*, *40*(5), pp.7417-7424., doi: 10.1016/j.ceramint.2013.12.088.

[11] Kathiresan, G., Vijayakumar, K., Sundarrajan, A.P., Kim, H.S. and Adaikalam, K., 2021. Photocatalytic degradation efficiency of ZnO, GO and PVA nanoadsorbents for crystal violet, methylene blue and trypan blue dyes. *Optik*, *238*, p.166671, doi: 10.1016/j.ijleo.2021.166671.

[12] Bilici, Z., Işık, Z., Aktaş, Y., Yatmaz, H.C. and Dizge, N., 2019. Photocatalytic effect of zinc oxide and magnetite entrapped calcium alginate beads for azo dye and hexavalent chromium removal from solutions. *Journal of Water Process Engineering*, *31*, p.100826, doi: 10.1016/j.jwpe.2019.100826.

[13] Chavan, R.R., More, V.R., Pawar, N.V., Dawkar, V.V., Jadhav, J.P., Patil, R.B. and Chougale, A.D., 2024. Catalytic and kinetic studies of CuFe2O4 as a superior heterogeneous nanocatalyst for dye degradation and Cr (VI) reduction. *Clean Technologies and Environmental Policy*, pp.1-21, doi: 10.1007/s10098-023-02727-5.

[14] Sanakousar, M.F., CC, V., Jiménez-Pérez, V.M., Jayanna, B.K., Shridhar, A.H. and Prakash, K., 2021. Efficient photocatalytic degradation of crystal violet dye and electrochemical performance of modified MWCNTs/Cd-ZnO nanoparticles with quantum chemical calculations. *Journal of Hazardous Materials Advances*, *2*, p. 100004, doi: 10.1016/j.hazadv.2021.100004.

[15] González-Casamachin, D.A., De la Rosa, J.R., Lucio-Ortiz, C.J., De Rio, D.A.D.H., Martínez-Vargas, D.X., Flores-Escamilla, G.A., Guzman, N.E.D., Ovando-Medina, V.M. and Moctezuma-Velazquez, E., 2019. Visible-light photocatalytic degradation of acid violet 7 dye in a continuous annular reactor using ZnO/PPy photocatalyst: Synthesis, characterization, mass transfer effect evaluation and kinetic analysis. *Chemical Engineering Journal*, *373*, pp.325-337, doi: 10.1016/j.cej.2019.05.032.

[16] Chavan, R., Bhat, N., Parit, S., Narasimharao, K., Devan, R.S., Patil, R.B., Karade, V.C., Pawar, N.V., Kim, J.H., Jadhav, J.P. and Chougale, A.D., 2023. Development of magnetically recyclable nanocatalyst for enhanced Fenton and photo-Fenton degradation of MB and Cr (VI) photo-reduction. *Materials Chemistry and Physics*, *293*, p.126964, doi: 10.1016/j.matchemphys.2022.126964.

[17] Hassan, N., Shahat, A., El-Didamony, A., El-Desouky, M.G. and El-Bindary, A.A., 2020. Synthesis and characterization of ZnO nanoparticles via zeolitic imidazolate framework-8 and its application for removal of dyes. *Journal of molecular structure*, *1210*, p.128029, doi: 10.1016/j.molstruc.2020.128029.

[18] Saeed, M., Albalawi, K., Khan, I., Akram, N., Abd El-Rahim, I.H., Alhag, S.K. and Ahmed, A.E., 2023. Synthesis of pn NiO-ZnO heterojunction for photodegradation of crystal violet dye. *Alexandria Engineering Journal*, *65*, pp.561-574, doi: 10.1016/j.aej.2022.09.048.

[19] Puneetha, J., Kottam, N. and Rathna, A., 2021. Investigation of photocatalytic degradation of crystal violet and its correlation with bandgap in ZnO and ZnO/GO nanohybrid. *Inorganic Chemistry Communications*, *125*, p.108460, doi: 10.1016/j.inoche.2021.108460.

[20] Jadhav, A., Chavan, R., Sonawane, S., Kamble, P., Mahajan, S., Vhankhande, B., Ghorpade, R., Chougale,

A., Abd El-Salam, N.M., Fouad, H. and Patil, R., 2024. Photocatalytic Degradation of Crystal Violet Dye Using Iron Oxide Nanoparticles. *Journal of Nanoelectronics and Optoelectronics*, *19*(3), pp.272-277, 2024, doi: 10.1166/jno.2024.3571.

[21] Siddiqi, K.S., Ur Rahman, A., Tajuddin, N. and Husen, A., 2018. Properties of zinc oxide nanoparticles and their activity against microbes. *Nanoscale Research Letters*, *13*, pp.1-13, doi: 10.1186/s11671-018-2532-3.

[22] Manohar, A., Park, J., Geleta, D.D., Krishnamoorthi, C., Thangam, R., Kang, H. and Lee, J., 2021. Synthesis and characterization of ZnO nanoparticles for photocatalysis, antibacterial and cytotoxicity in kidney cancer (A498) cell lines. *Journal of Alloys and Compounds*, *874*, p.159868, doi: 10.1016/j.jallcom.2021.159868.

[23] Pascariu, P., Tudose, I.V., Suchea, M., Koudoumas, E., Fifere, N. and Airinei, A., 2018. Preparation and characterization of Ni, Co doped ZnO nanoparticles for photocatalytic applications. *Applied Surface Science*, *448*, pp.481-488, doi: 10.1016/j.apsusc.2018.04.124.

[24] T. Terasako, N. A. Hambali, N. A. Jayah, T. Wakisaka, A. M. Hashim, and M. Yagi, Shape controlled growth of ZnO nanorods and fabrication of ZnO/CuO heterojunctions by chemical bath deposition using zinc nitrate hexahydrate and copper (III) nitrate trihydrate, *Thin Solid Films*, vol. 596, pp. 201–208, 2015, doi: 10.1016/j.tsf.2015.07.082.

[25] Zhang, Y.L., Yang, Y., Zhao, J.H., Tan, R.Q., Cui, P. and Song, W.J., 2009. Preparation of ZnO nanoparticles by a surfactant-assisted complex sol–gel method using zinc nitrate. *Journal of Sol-Gel Science and Technology*, *51*, pp.198-203., doi: 10.1007/s10971-009-1959-5.

[26] Zhao, X., Lee, J.Y., Kim, C.R., Heo, J., Shin, C.M., Leem, J.Y., Ryu, H., Chang, J.H., Lee, H.C., Jung, W.G. and Son, C.S., 2009. Dependence of the properties of hydrothermally grown ZnO on precursor concentration. *Physica E: Low-dimensional Systems and Nanostructures*, *41*(8), pp.1423-1426., doi: 10.1016/j.physe.2009.04.012.

[27] Davar, F., Majedi, A. and Mirzaei, A., 2015. Green synthesis of ZnO nanoparticles and its application in the degradation of some dyes. *Journal of the American Ceramic Society*, *98*(6), pp.1739-1746., doi: 10.1111/jace.13467.

[28] Otero-González, L., Field, J.A. and Sierra-Alvarez, R., 2014. Fate and long-term inhibitory impact of ZnO nanoparticles during high-rate anaerobic wastewater treatment. *Journal of environmental management*, *135*, pp.110-117., doi: 10.1016/j.jenvman.2014.01.025.

[29] Gu, M., Hao, L., Wang, Y., Li, X., Chen, Y., Li, W. and Jiang, L., 2020. The selective heavy metal ions adsorption of zinc oxide nanoparticles from dental wastewater. *Chemical Physics*, *534*, p.110750., doi: 10.1016/j.chemphys.2020.110750.

[30] Janaki, A.C., Sailatha, E. and Gunasekaran, S., 2015. Synthesis, characteristics and antimicrobial activity of ZnO nanoparticles. *Spectrochimica Acta Part A: Molecular and Biomolecular Spectroscopy*, *144*, pp.17-22, doi: 10.1016/j.saa.2015.02.041.

[31] Chavan, R., Mujawar, S., Dawkar, V., More, V., Pawar, N., Patil, R., Jadhav, J., Mustafa, J., Jameel, B., Muhaisen, H.M. and Mohammed, A.Y., 2024. Enhanced Photodegradation of Methylene Blue Using Reusable Cobalt Ferrite Nanocomposites. *Science of Advanced Materials*, *16*(5), pp.589-595, doi: 10.1166/sam.2024.4689.

[32] Chavan, R. R., Rathod, K. C., More, V. R., Pawar, N.V., Jadhav, J. P., Patil, R. B. and Chougale, A. D. 2024, Catalytic Activity of CuO-bentonite Bead for the Removal of Methylene Blue by Fenton like Process. MatSci Express 1(2), pp. 96-104; https://doi.org/10.69626/mse.2024.0096.

